Validity of the Measured Equation of Invariance

Yun-Sheng Xu, *Member, IEEE*, and Hong-Ming Chen

***Abstract*—The measured equation of invariance (MEI) is derived without any postulates. It is shown that the coefficients of the MEI are invariant to the field of excitation. However, the accuracy of the MEI solution is closely related to the number of nodes in the MEI. Coupling more nodes improves progressively the accuracy of the MEI solution. With increasing nodes, the matrix problem for the determination of the MEI coefficients becomes seriously ill conditioned and generally must be solved using multiple precision arithmetic. The consequences of the ill-conditioning phenomenon are discussed.**

***Index Terms*— Electromagnetic wave scattering, finite-difference method, measured equation of invariance.**

I. Introduction

THE measured equation of invariance (MEI) [1] is a newly developed numerical method that may, if correct and practical, truncate a finite-difference (FD) or a finite-element mesh (FEM) very close to the object boundary in the analysis of scattering problems. It has been applied to a variety of field problems [1]–[20]. Since the MEI method is formulated based on postulates and lack of theoretical foundations, there have been conflicts on the validity of the method since its appearance [21]–[27]. The major controversies lie in the validity of the postulate of the invariance of the MEI to the field of excitation, the dependency of the accuracy of the MEI solution on the mesh size, etc. These subjects are addressed in this paper.

More recently, Xu derived the MEI without any postulates and came to the following conclusions [28]: the coefficients of the MEI are indeed invariant to the field of excitation; on the other hand, the accuracy of the MEI solution is closely related to the number of nodes in the MEI. Coupling more nodes may improve progressively the accuracy of the MEI solution. The detailed derivation and related discussions in [28] are given in Section II of this paper. With increasing nodes in the MEI, the matrix used to determine the MEI coefficients becomes seriously ill conditioned. Although the ill-conditioning phenomenon has been mentioned in previous publications [6], [9], [25], its severe consequences have not been sufficiently recognized and the necessity and the way to overcome this difficulty have not been pointed out. Hence, an intensive investigation is presented in Section III. Multiple precision arithmetic (MPA) [29] is eventually used to solve this problem. It was demonstrated in [25] that the error of the MEI solution cannot be reduced below a certain limit no matter how dense the mesh is if a six-node MEI is used. We show through calculation of the scattering by perfectly conducting circular cylinders in Section III that coupling more nodes in the MEI may improve progressively the accuracy of the solution. Also in Section III, we discuss the numerical method suitable to the solution of the overall FD-MEI matrix equation and show the fast decaying behavior of the residual of the MEI. In Section IV, we discuss the consequences of the matrix ill-conditioning phenomenon encountered in the computation of MEI coefficients.

Manuscript received July 21, 1998; revised May 25, 1999.

Y.-S. Xu is with the Department of Electronic Engineering and Information Science, University of Science and Technology of China, Hefei, Anhui, 230027 China.

H.-M. Chen is with the Huawei Technologies Corporation, Ltd., Shenzhen, Guangdong, 518057 China.

Publisher Item Identifier S 0018-926X(99)09983-4.

II. Derivation of the MEI

In this section, the MEI is derived for the problem of electromagnetic wave scattering by a perfectly conducting cylinder. For the case of a TM wave incidence, the longitudinal electric field component φ of the scattered field can be expressed as

$$\varphi = -j\omega\mu_0 \int_\Gamma G(\vec{\rho},\vec{\rho}')K_z(\vec{\rho}')\,d\ell' \tag{1}$$

where $\vec{\rho}$ and $\vec{\rho}'$ are the position vectors to the field and source points, respectively, Γ is the contour of the cylinder, $J_z(\vec{\rho}')$ is the induced longitudinal electric surface current density on the cylinder, and $G(\vec{\rho},\vec{\rho}')$ is the two-dimensional free-space Green's function given by

$$G(\vec{\rho},\vec{\rho}') = \frac{1}{4j}H_0^{(2)}(k|\vec{\rho}-\vec{\rho}'|) \tag{2}$$

with $k = 2\pi/\lambda$ being the free-space wavenumber and $H_0^{(2)}$ being the Hankel function of the second kind of order zero. In order to derive a discretized form of (1) at, say, node 0 on the mesh truncation boundary, J_z is expanded in terms of a complete set of basis functions defined on the surface of the cylinder $\{f_n(\vec{\rho}'), n = 1,2,\cdots\}$

$$J_z(\vec{\rho}') = \sum_{n=1}^{N} c_n f_n(\vec{\rho}') \tag{3}$$

where c_n's are the current expansion coefficients. This expression is exact if N becomes infinite. Substitution of (3) into (1) yields

$$\varphi = -j\omega\mu_0 \sum_{n=1}^{N} c_n \int_\Gamma G(\vec{\rho},\vec{\rho}')f_n(\vec{\rho}')\,d\ell'. \tag{4}$$

Hence, we have the following equation at node 0:

$$\varphi_0 = [b_0]^t[c] \tag{5}$$

where the superscript t denotes the matrix transposition. $[b_0]$ and $[c]$ are column vectors defined as

$$[b_0]^t = [b_{10}, b_{20}, \cdots, b_{N0}] \tag{6}$$

$$[c]^t = [c_1, c_2, \cdots, c_N] \tag{7}$$

with b_{n0} given by

$$b_{n0} = -j\omega\mu_0 \int_\Gamma G(\vec{\rho}_0, \vec{\rho}\,')f_n(\vec{\rho}\,')\, d\ell' \tag{8}$$

where $\vec{\rho}_0$ is the position vector to node 0. The unknown current expansion coefficients c_n's in (4) or (5) can be expressed as linear combinations of the values of φ at N nodes, locally numbered 1 to N in the immediate neighbor of node 0; and the discretized form of (1) at node 0 can be derived in this way. Use of (4) again at these N nodes gives

$$\varphi_m = \sum_{n=1}^{N} b_{nm}c_n, \qquad m = 1, 2, \cdots, N \tag{9}$$

where φ_m is the value of φ at node m and the definition of b_{nm} is the same as (8) except that $\vec{\rho}_0$ is replaced by $\vec{\rho}_m$, the position vector to node m. In matrix form, (9) can be written as

$$[\varphi] = [B]^t[c] \tag{10}$$

where $[\varphi]$ is a column vector given by

$$[\varphi]^t = [\varphi_1, \varphi_2, \cdots, \varphi_N] \tag{11}$$

and $[B]$ is a square matrix of order N whose elements are b_{nm} $(n, m = 1, 2, \cdots, N)$. From (10), one can obtain $[c] = \{[B]^t\}^{-1}[\varphi]$ and its substitution into (5) results in the following discretized form of (1) at node 0:

$$\varphi_0 = [b_0]^t\{[B]^t\}^{-1}[\varphi] = \{[B]^{-1}[b_0]\}^t[\varphi]. \tag{12}$$

We will show that this is actually the MEI at node 0 and the procedures in [1] to obtain the MEI are equivalent to the above way of discretization of (1).

The MEI method postulates the validity of the following equation at node 0:

$$\sum_{m=0}^{N} a_m\varphi_m = 0. \tag{13}$$

Since one of these coefficients a_m's may be arbitrary, we can simply let $a_0 = -1$. The rest a_m's can be determined through N measures. If the same basis functions $\{f_n(\vec{\rho}\,'), n = 1, 2, \cdots, N\}$ are chosen as metrons, the value of the nth measuring function at node m is then b_{nm} $(m = 0, 1, 2, \cdots, N)$ and the N measures are

$$\begin{aligned} b_{10} &= \sum_{m=1}^{N} a_m b_{1m} \\ b_{20} &= \sum_{m=1}^{N} a_m b_{2m} \\ &\cdots\cdots\cdots\cdots\cdots\cdots \\ b_{N0} &= \sum_{m=1}^{N} a_m b_{Nm}. \end{aligned} \tag{14}$$

Using matrix notation, (13) and (14) can be respectively rewritten as

$$\varphi_0 = [a]^t[\varphi] \tag{15}$$

$$[b_0] = [B][a] \tag{16}$$

where $[a]$ is a column vector given by

$$[a]^t = [a_1, a_2, \cdots, a_N]. \tag{17}$$

Substituting $[a] = [B]^{-1}[b_0]$ derived from (16) into (15), one obtains exactly the same equation as (12).

For the case of a TE wave incidence, the MEI can be similarly derived. The only differences are: φ represents now the longitudinal magnetic field component; φ and correspondingly b_{nm} have other integral expressions. Obviously, the present derivation of the MEI can also be extended to the three-dimensional case.

Thus, we have derived the MEI without any postulates. It is seen that the linear relation among the discrete field value at a node on the mesh truncation boundary and those at its immediate neighbors, namely the MEI, does exist. But it can be derived and does not need to appear as a postulate as in the original MEI method [1]. The coefficients of the MEI are invariant to the field of excitation because the incident field affects the current expansion coefficients c_n's only which do not appear in the MEI nor in (16) used to determine the MEI coefficients.

The only approximation in the above derivation exists in (1) when N is finite. If N becomes infinite, the MEI is exact. For finite N, the MEI can only be approximately valid. This implies that commonly used four-, six-, or, at most, eight-node MEI may not be able to provide sufficiently accurate results in any case. Numerical computations in [25] and here show that this is indeed the situation, especially for electrically large cylinders. However, it will be demonstrated through numerical results in the next section that using a sufficient number of nodes in the MEI and a sufficiently fine mesh, one may obtain the MEI solution with desired order of accuracy.

It is well known that the MEI with small N cannot produce accurate numerical results for concave structures [14]. We believe that with a sufficiently large N one may also obtain rigorous results for this kind of structures.

III. Numerical Results and Discussions

Numerical results for perfectly conducting circular cylinders are presented in this section. The nodal configuration of the MEI is shown in Fig. 1. The amplitude of the incident plane wave is assumed to be unity. Harmonic basis functions $e^{jn\theta}$ $(n = 0, 1, 2, \cdots)$ are chosen as metrons. The analytical expressions of the corresponding measuring functions for TM waves are available [25]

$$\begin{aligned} &-\tfrac{1}{2}\pi ka\eta J_n(ka)H_n^{(2)}(k\rho)e^{jn\theta} \\ &\qquad \rho > a, \qquad n = 0, \pm 1, \pm 2, \cdots \end{aligned} \tag{18}$$

where η is the wave impedance of free-space and J_n and $H_n^{(2)}$ are Bessel function of the first kind and Hankel function of the second kind, respectively. For TE waves, the analytical

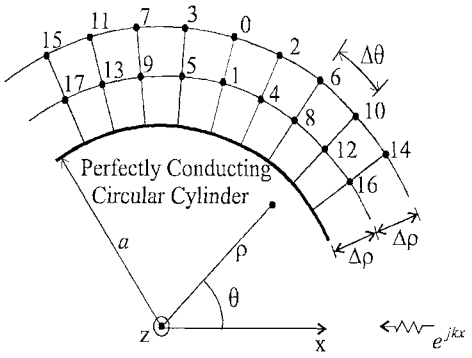

Fig. 1. Nodal configuration and local numbering of the MEI $(N = 17)$.

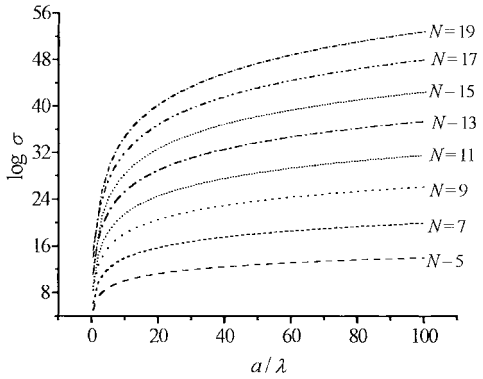

Fig. 2. Logarithm of the condition number σ versus the electric size of the cylinder for various N. $\Delta\rho = \lambda/40, \Delta\theta = \Delta\rho/a$.

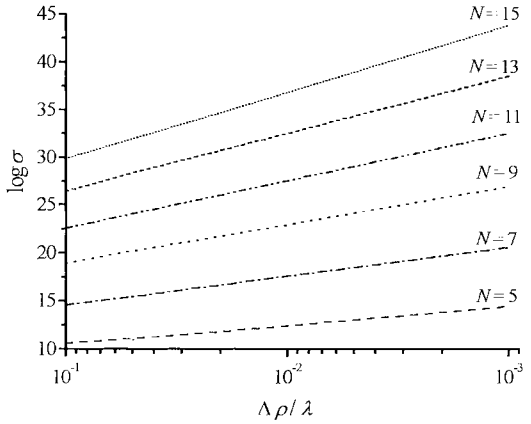

Fig. 3. Logarithm of the condition number versus the mesh density for various N. $a = 25\lambda, \Delta\theta = \Delta\rho/a$.

expressions of the measuring functions can also be derived as follows:

$$\frac{j}{2}\pi ka J_n'(ka) H_n^{(2)}(k\rho) e^{jn\theta} \qquad \rho > a, \qquad n = 0, \pm 1, \pm 2, \cdots. \tag{19}$$

It is easily seen that the MEI coefficients are actually the same for both TM and TE waves. Besides, with the symmetric nodal distribution of the MEI as in Fig. 1, the MEI coefficients can be determined independent of its location on the mesh truncation boundary.

A. Ill Conditioning of the Matrix

The matrix $[B]$ in (16) used to solve for the MEI coefficients becomes seriously ill conditioned for N, which is larger than about seven. The 64-bit double precision arithmetic (DPA) available on our personal computer cannot provide accurate results for the MEI coefficients in this case. We apply MPA [29] to tackle this problem.

Mathematically, the ill conditioning of a matrix is described by the order of its condition number. The dependence of the condition number σ of the matrix $[B]$ on N, the electric size of the cylinder, and the mesh density is shown in Figs. 2 and 3. The results are obtained by the singular value decomposition (SVD) with MPA and the condition number is equal to the ratio of the largest and the smallest singular values. As can be seen from the figures, the matrix $[B]$ becomes more ill-conditioned as the electric size of the cylinder becomes larger, the mesh size decreases, and N increases. The condition number changes most drastically with varying N.

The inverse of the condition number of a matrix actually represents the order of the required minimum floating-point accuracy to guarantee a rigorous solution for the matrix problem. For the case in Fig. 2, the condition number is about 10^{30} when $a = 25\lambda$ and $N = 13$; all procedures of the numerical computation related to the determination of the MEI coefficients should then be more accurate than 10^{-30}. In other words, to obtain accurate results for the MEI coefficients, all the numerical processes concerned should retain more than 30 significant decimal digits, which clearly goes beyond the limitation of 64-bit DPA. Although on some workstations or supercomputers 128-bit DPA is available, its ability to deal with the present ill-conditioned matrix is still very limited. The MPA in [29] may provide as many significant digits as desired, it is, therefore, used to determine the MEI coefficients.

To show the effect of the matrix ill conditioning on the accuracy of the computed MEI coefficients, we present (in Table I) some numerical results obtained by SVD and Gauss–Jordanian elimination (GJE) with DPA and MPA. Those calculated by SVD and GJE with MPA coincide with each other. The situation is different, if 64-bit DPA is used. For $N = 5$, both SVD-DPA and GJE-DPA may provide sufficiently accurate MEI coefficients—about five accurate decimal digits. Even in this case, the effect of the matrix ill conditioning can also be seen. If a well-conditioned matrix problem of such a small order as 5×5 is to be solved, one may expect the 64-bit DPA on our personal computer to provide the results with about 16 accurate decimal digits. For $N = 7$, the results calculated by GJE-DPA become inaccurate. SVD-DPA works better than GJE-DPA, but generates only two or three accurate decimal digits. For $N = 9$, both GJE-DPA and SVD-DPA give completely wrong results. The reason can be easily found through the condition number of the matrix $[B]$. For the case in Table I, we have also used the conjugate gradient method with DPA to solve for the MEI coefficients, but succeeded in obtaining similar accurate results as those generated by GJE and SVD with DPA for $N = 5$ only. For $N = 7$ or 9, either the results were inaccurate or the iteration did not converge.

TABLE I
MEI COEFFICIENTS CALCULATED BY GJE AND SVD WITH DPA AND MPA ($a_0 = -1$). $a = 25\lambda, \Delta\rho = \lambda/40, \Delta\theta = \Delta\rho/a$

N	σ	a_m	DPA		MPA
			GJE	SVD	GJE or SVD
5	10^{11}	a_1	.88186551-.46120874j	.88184253-.46122952j	.88186708-.46121710j
		a_2	.52500209-.00459991j	.52500340-.00460145j	.52500274-.00459969j
		a_3	.52500211-.00459992j	.52500399-.00460147j	.52500274-.00459969j
		a_4	-.46489547+.23905463j	-.46488562+.23906684j	-.46489693+.23905870j
		a_5	-.46489549+.23905465j	-.46488561+.23906686j	-.46489694+.23905870j
7	10^{16}	a_1	-.04215176+.17477537j	.10189516-.17344509j	.10153021-.17271612j
		a_2	.67810631-.02198604j	.66047099-.03091431j	.66046528-.03080012j
		a_3	.67786570-.02151188j	.66046550-.03090967j	.66046528-.03080012j
		a_4	.02316122-.08876620j	-.05230450-.08892341j	-.05211710-.08853890j
		a_5	.02324291-.08875384j	-.05230354-.08892283j	-.05211710-.08853890j
		a_6	-.18034232+.02289709j	-.15947342+.03330020j	-.15947059+.03316679j
		a_7	-.18026140+.02264751j	-.15947110+.03329752j	-.15947059+.03316679j
9	10^{21}	a_1	-1.2771560+1.8005069j	1.0348164-.13129329j	.67915859-.71533551j
		a_2	-.19858235+1.6255204j	1.8253107+.79885158j	.68196382-.00476563j
		a_3	1.4282420-1.8076766j	-.61897434-.88625720j	.68196382-.00476563j
		a_4	.85583532-3.0217269j	-2.0792290-.86268349j	-.46620690+.48551612j
		a_5	1.0037300+.75639331j	.85286772+.27337071j	-.46620690+.48551612j
		a_6	.31001036-.80679575j	-.73643480-.38770149j	-.18274431+.00508793j
		a_7	-.52828826+1.0030518j	.55450659+.48568135j	-.18274431+.00508793j
		a_8	-.26594512+1.2188467j	.85229126+.06853226j	.12734771-.12828858j
		a_9	-.32990481-.76615964j	.55450659+.48568135j	.12734771-.12828858j

B. Solution of the Overall FD-MEI Matrix Equation

Iterative methods are commonly utilized to solve large sparse matrices. At the early stage of our work, we also tried to apply (with DPA) various iterative methods such as the conjugate gradient method, preconditioned biconjugate gradient method, Jacobi semi-iterative method, successive overrelaxation, and so on, to the solution of the overall FD-MEI matrix equation. If few nodes, e.g. six nodes ($N = 5$), are coupled in the MEI, they all work well, although some of them may run faster than the others. Unfortunately, all of them presented great difficulty in achieving the convergence of iteration, as the number of nodes in the MEI increases. A finer mesh or an electrically larger cylinder makes the situation even worse. After many painful efforts with various iterative methods, the authors finally decided to use a sparse matrix solver "Y12M," which utilizes a direct method—LU decomposition with Gaussian elimination. It works well and very fast. For the examples in the next part, solving a FD-MEI matrix equation on our personal computer (233MHz Pentium II) takes 5–60 s, depending on the situation.

Although we have not carried out intensive investigations as in the preceding part, it is believed that the condition number of the overall FD-MEI matrix increases as more nodes are coupled in the MEI. Nevertheless, the problem is less serious than in the preceding part, as far as the remainder of this paper is concerned. Otherwise, we could not have obtained with 64-bit DPA the rigorous results to be presented in the next part.

C. Scattering by Circular Cylinders

Now we present some numerical results for the scattering by circular cylinders obtained by the MEI together with the FD method. The results are always calculated with sufficiently small (often unnecessarily small) mesh sizes so that any finer mesh will not make any significant difference, at least within the error of graphic illustrations. For a cylinder of radius 25λ, it was demonstrated in [25] that the error of the MEI solution for the case of a TM wave incidence cannot be reduced below a certain limit no matter how dense the mesh is if a six-node MEI ($N = 5$) is used. We have obtained the same results. It is shown in Figs. 4 and 5 for TM and TE waves, respectively, however, that using more nodes in the MEI may progressively reduce the error. In Figs. 6 and 7, the induced surface current densities for the cylinder of radius 50λ computed with various N are depicted for TM and TE waves, respectively. Again, the MEI solutions become more and more accurate as N increases.

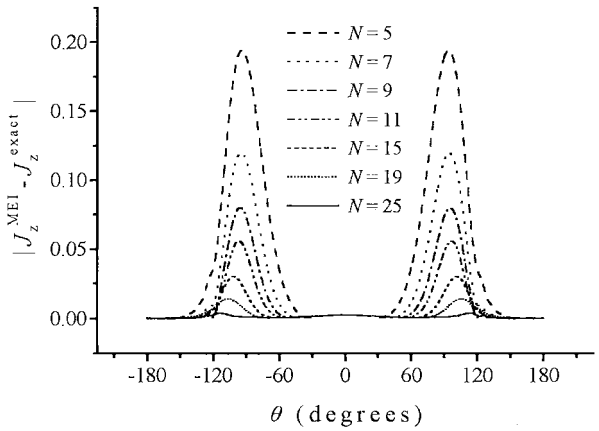

Fig. 4. Error of the MEI solution for the induced TM surface current density J_z. $a = 25\lambda, \Delta\rho = \lambda/80, \Delta\theta = 0.08°$.

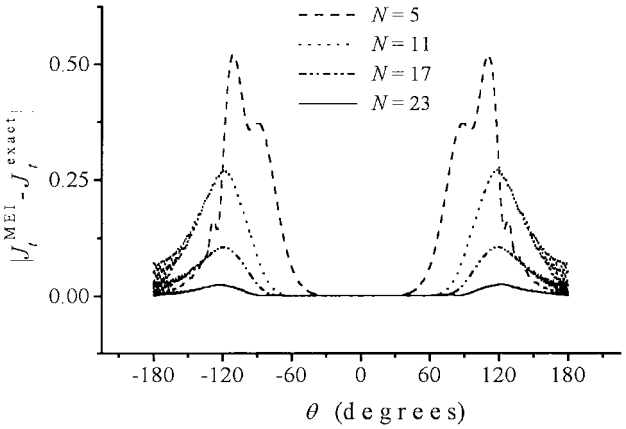

Fig. 5. Error of the MEI solution for the induced TE surface current density J_t. $a = 25\lambda, \Delta\rho = \lambda/40, \Delta\theta = 0.08°$.

The numerical results here show clearly that the MEI is very different from the conventional finite-difference equations. The error produced by the finite-difference approximation of a differential equation can be reduced to zero as the mesh size goes to zero. Apparently, this is not the case for the MEI with a fixed finite N as an approximation of the exact mesh truncation boundary condition.

D. Residual of the MEI

In this section, we discuss the residual of the MEI caused by a finite N and defined as

$$\sum_{m=0}^{N} a_m \varphi_m = R \qquad (a_0 = -1). \tag{20}$$

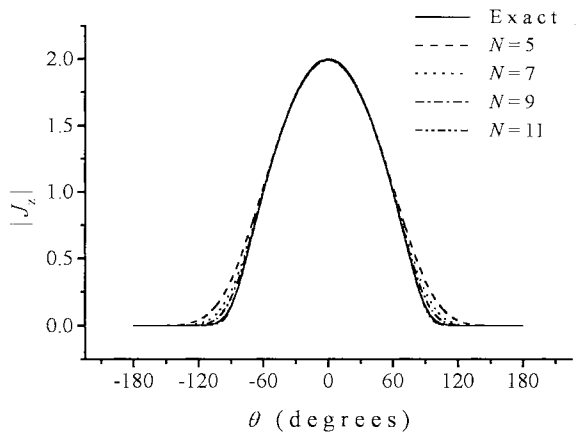

Fig. 6. Amplitude of the induced TM surface current density J_z calculated by the MEI method and comparison with the exact solution. $a = 50\lambda, \Delta\rho = \lambda/40, \Delta\theta = 0.05°$.

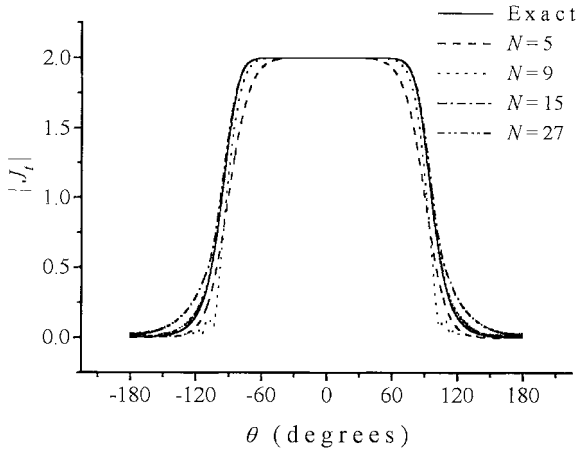

Fig. 7. Amplitude of the induced TE surface current density J_t calculated by the MEI method and comparison with the exact solution. $a = 50\lambda, \Delta\rho = \lambda/40, \Delta\theta = 0.05°$.

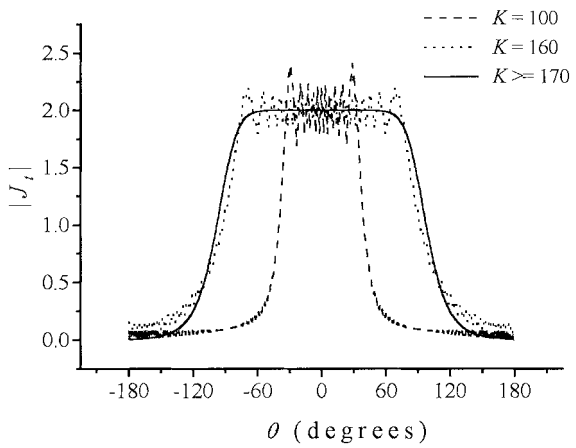

Fig. 8. Analytical solution of the induced TE surface current density J_t expressed in terms of harmonic functions $e^{jn\theta}$ with n up to $\pm K$. $a = 25\lambda$.

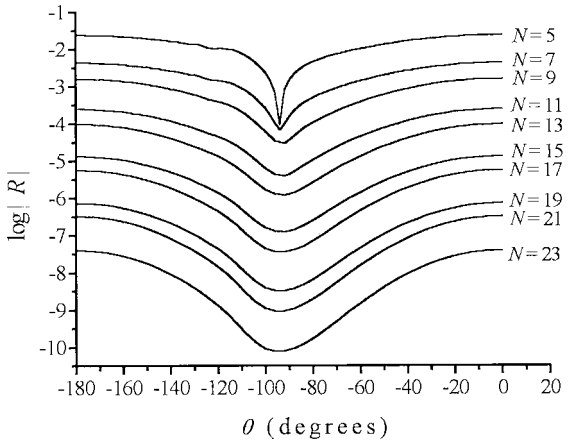

Fig. 9. Logarithm of the residual of the MEI under a TE plane wave incidence for various N. $a = 25\lambda, \Delta\rho = \lambda/40, \Delta\theta = 0.08°$.

The exact analytical solution for circular cylinders can be expressed as a series in terms of harmonic functions $e^{jn\theta}$. To obtain accurate results for the case in Fig. 5 about $N = 341$ (n up to ± 170) terms must be taken into account, as illustrated in Fig. 8. On the contrary, if the problem is solved by the MEI method, $N = 23$ (n up to ± 11) is large enough to generate a rigorous solution. Our explanation is that although both (3) and (12) or (13) are truncated behind the Nth basis function, the truncation errors or the residuals do not necessarily have the same asymptotic behavior with respect to N. In fact, we believe that the residual of the MEI decays much faster to zero than that of (3). To demonstrate this, we show in Fig. 9 the residual of the MEI for various N obtained by substituting the exact analytical solution into (20). It can be seen that the residual of the MEI approaches very rapidly to zero as N becomes large. Changing N from 5 to 23 makes the residual of the MEI about six orders of magnitude lower. Although theoretically N should approach infinity to make the MEI exact, due to the fast decaying of its residual, only a small number of basis functions need to be taken into account in practice, even if any linear combination of these basis functions may be far from being sufficient to express accurately the surface current density. It is this property of the MEI that allows one use much less basis functions than in analytical methods or the moment method so as to preserve still-good sparsity of the overall FD-MEI matrix though not so sparse as FD or finite-element matrices. Otherwise, the MEI method would have no merits.

IV. Consequences of the Ill-Conditioning Phenomenon of the Matrix $[B]$

We have shown in the preceding section that the matrix problem (16) is ill conditioned for large N and MPA must generally be used to obtain accurate results for MEI coefficients. MPA is much slower than DPA. For a circular cylinder, since the analytical expressions for the measuring functions are available and the MEI coefficients for each node on the mesh truncation boundary are the same, this problem is not serious. For electrically large cylinders of arbitrary cross section, however, one must generally carry out numerical integration with very high accuracy at various locations on the mesh truncation boundary; even worse is that the required accuracy increases drastically as the nodes in the MEI become more

and the computation time would be eventually unacceptable. This is also the reason why only numerical results for circular cylinders are presented here. Consequently, although the MEI method in its original form [1] is correct, provided a sufficient number of nodes are used in the MEI, further investigations must be carried out on the accurate and efficient calculation of the MEI coefficients before the MEI method can generally be used as a practical and efficient full wave numerical method for scattering problems.

REFERENCES

[1] K. K. Mei, R. Pous, Z. Chen, Y.-W. Liu, and M. D. Prouty, "Measured equation of invariance: A new concept in field computations," *IEEE Trans. Antennas Propagat.*, vol. 42, pp. 320–328, Mar. 1994.

[2] A. C. Cangellaris and D. B. Wright, "Application of the measured equation of invariance to electromagnetic scattering by penetrable bodies," *IEEE Trans. Magn.*, vol. 29, pp. 1628–1631, Mar. 1993.

[3] R. Gordon, R. Mittra, A. Glisson, and E. Michielssen, "Finite element analysis of electromagnetic scattering by complex bodies using an efficient numerical boundary condition for mesh truncation," *Electron. Lett.*, vol. 29, no. 12, pp. 1102–1103, June 1993.

[4] M. D. Prouty, K. K. Mei, S. E. Schwarz, and R. Pous, "A new approach to quasistatic analysis with application to microstrip," *IEEE Microwave Guided Wave Lett.*, vol. 3, pp. 302–304, Sept. 1993.

[5] A. Boag, A. Boag, R. Mittra, and Y. Leviatan, "A numerical absorbing boundary condition for finite-difference and finite-element analysis of open structures," *Microwave Opt. Technol. Lett.*, vol. 7, no. 9, pp. 395–398, June 1994.

[6] T. L. Barkdoll and R. Lee, "Finite element analysis of bodies of revolution using the measured equation of invariance," *Radio Sci.*, vol. 30, no. 4, pp. 803–815, July/Aug. 1995.

[7] W. Hong, Y. Liu, and K. K. Mei, "Application of the measured equation of invariance to solve scattering problems involving a penetrable medium," *Radio Sci.*, vol. 29, no. 4, pp. 897–906, July/Aug. 1994.

[8] D. B. Wright and A. C. Cangellaris, "Finite element grid truncation schemes based on the measured equation of invariance," *Radio Sci.*, vol. 29, no. 4, pp. 907–921, July/Aug. 1994.

[9] R. Janaswamy, "A fast finite difference method for propagation predictions over irregular, inhomogeneous terrain," *IEEE Trans. Antennas Propagat.*, vol. 42, pp. 1257–1267, Sept. 1994.

[10] G. K. Gothard, S. M. Rao, T. K. Sarkar, and M. S. Palma, "Finite element solution of open region electrostatic problems incorporating the measured equation of invariance," *IEEE Microwave Guided Wave Lett.*, vol. 5, pp. 252–254, Aug. 1995.

[11] J. M. Rius, R. Pous, and A. Cardama, "Integral formulation of the measured equation of invariance: A novel sparse matrix boundary element method," *IEEE Trans. Magn.*, vol. 32, pp. 962–967, May 1996.

[12] Z. Chen, W. Hong, and W. Zhang, "Electromagnetic scattering from a chiral cylinder—General case," *IEEE Trans. Antennas Propagat.*, vol. 44, pp. 912–917, July 1996.

[13] J. M. Rius, C. P. Carpintero, A. Cardama, and J. R. Mosig, "Frequency extrapolation in the integral equation MEI," *Electron. Lett.*, vol. 32, no. 25, pp. 2324–2326, Dec. 1996.

[14] J. M. Rius, C. P. Carpintero, A. Cardama, and K. A. Michalski, "Analysis of electrically large concave scatterers with the integral equation MEI," *Microwave Opt. Technol. Lett.*, vol. 14, no. 5, pp. 287–289, Apr. 1997.

[15] W. Sun, W. W.-M. Dai, and W. Hong, "Fast parameter extraction of general interconnects using geometry independent measured equation of invariance," *IEEE Trans. Microwave Theory Tech.*, vol. 45, pp. 827–836, May 1997.

[16] J. Y. Zhou and W. Hong, "A super absorbing boundary condition for the analysis of waveguide discontinuities with the finite-difference method," *IEEE Microwave Guided Wave Lett.*, vol. 7, pp. 147–149, June 1997.

[17] Y. Zhao and Y.-Y. Wang, "A new finite-element solution for parameter extraction of multilayer and multiconductor interconnects," *IEEE Microwave Guided Wave Lett.*, vol. 7, pp. 156–158, June 1997.

[18] M. D. Prouty, K. K. Mei, S. E. Schwarz, R. Pous, and Y.-W. Liu, "Solving microstrip discontinuities by the measured equation of invariance," *IEEE Trans. Microwave Theory Tech.*, vol. 45, pp. 877–885, June 1997.

[19] Y.-W. Liu, E. K.-N. Yung, and K. K. Mei, "Interpolation, extrapolation, and application of the measured equation of invariance to scattering by very large cylinders," *IEEE Trans. Antennas Propagat.*, vol. 45, pp. 1325–1331, Sept. 1997.

[20] J. M. Rius, J. Parron, E. Ubeda, and J. R. Mosig, "Integral equation MEI applied to three-dimensional arbitrary surfaces," *Electron. Lett.*, vol. 33, no. 24, pp. 2029–2031, Nov. 1997.

[21] J. O. Jevtic and R. Lee, "A theoretical and numerical analysis of the measured equation of invariance," *IEEE Trans. Antennas Propagat.*, vol. 42, pp. 1097–1105, Aug. 1994.

[22] K. K. Mei, Y. Liu, J. O. Jevtic, and R. Lee, "Comments on 'A theoretical and numerical analysis of the measured equation of invariance,"' *IEEE Trans. Antennas Propagat.*, vol. 43, pp. 1168–1171, Oct. 1995.

[23] J. O. Jevtic and R. Lee, "How invariant is the measured equation of invariance?," *IEEE Microwave Guided Wave Lett.*, vol. 5, pp. 45–47, Feb. 1995.

[24] K. K. Mei, J. O. Jevtic, and R. Lee, "Comments on 'How invariant is the measured equation of invariance?,"' *IEEE Microwave Guided Wave Lett.*, vol. 5, p. 417, Nov. 1995.

[25] J. O. Jevtic and R. Lee, "An analytical characterization of the error in the measured equation of invariance," *IEEE Trans. Antennas Propagat.*, vol. 43, pp. 1109–1115, Oct. 1995.

[26] K. M. Luk, E. K. N. Yung, K. W. Leung, and Y. W. Liu, "On the measured equation of invariance for an electrically large cylinder," *IEEE Microwave Guided Wave Lett.*, vol. 5, pp. 445–447, Dec. 1995.

[27] J. M. Rius, C. P. Carpintero, A. Cardama, and J. R. Mosig, "Theoretical error in the integral equation MEI," *Electron. Lett.*, vol. 32, no. 23, pp. 2131–2132, Nov. 1996.

[28] Y.-S. Xu, "Derivation of the measured equation of invariance," presented at *Res. Meet. Appl. Electromagn. Lab.*, Dept. Elect. Eng. Inform. Sci., Univ. Sci. Technol. China, Hefei, Anhui, June 1997.

[29] D. M. Smith, "A FORTRAN package for floating-point multiple-precision arithmetic," *ACM Trans. Math. Softw.*, vol. 17, no. 2, pp. 273–283, June 1991.

Yun-Sheng Xu (M'93) was born in Jiangsu Province, China, on November 29, 1961. He received the B.S. and M.S. degrees in engineering from the University of Science and Technology of China (USTC), Hefei, Anhui, in 1982 and 1985, respectively, and the Ph.D. degree in engineering from the Technische Universität Hamburg-Harburg, Germany, in 1993.

From 1984 to 1988, he was with the Department of Electronic Engineering and Information Science at the USTC as an Assistant and later as a Lecturer. Since 1994 he has been with the same department, where he is now an Associate Professor. His current research interests are in the areas of computational electromagnetics, electromagnetic wave scattering, and planar circuits.

Hong-Ming Chen, photograph and biography not available at the time of publication.